Available online at www.sciencedirect.com
ScienceDirect
Talanta 74 (2007) 370–375
Talanta
www.elsevier.com/locate/talanta

Biomolecules-carbon nanotubes doped conducting polymer nanocomposites and their sensor application

Maxwell C. Kum [1], Kanchan A. Joshi [1], Wilfred Chen, Nosang V. Myung, Ashok Mulchandani *

Department of Chemical and Environmental Engineering, and Center for Nanoscale Science and Engineering, University of California, Riverside, CA 92521, United States

Available online 14 September 2007

Published in honor of Professor Joseph Wang's 60th birthday.

Abstract

A simple method for preparing bio-functionalized soluble single-walled carbon nanotubes (SWNTs) is described. Different proteins such as bovine serum albumin (BSA), cytochrome *c* and horseradish peroxidase (HRP) were used to solubilize low functionality SWNTs in water aided by sonication. The unbound proteins were removed by column chromatography and the SWNT-protein conjugate was used as the sole anionic dopant in electropolymerization of polypyrrole from polymerization solution at pH above the isoelectric point of the protein to provide a negative charge. The morphology of the polypyrrole with SWNT-protein dopant was found to be three-dimensional and fibrous with wide open interlocking pores in contrast to smooth and cauliflower-like for chloride doped polypyrrole. Enhanced sensor performance was demonstrated for hydrogen peroxide detection on polypyrrole/SWCNT-HRP nanocomposites modified electrode. Such nanocomposites can be potentially applied for other biosensor and bio-fuel cell applications.

Keywords: Carbon nanotubes; Biomolecule; Conducting polymer; Polypyrrole; Nanocomposite; Biosensor

1. Introduction

Carbon nanotubes (CNTs) exhibit unique electronic, metallic, and structural characteristics [1]. Due to these interesting properties there are reports in literature about the sensor applications of CNTs [2,3]. CNTs show electrocatalytic activity toward biologically important compounds such as dopamine, epinephrine, and ascorbic acid [4], NADH [5], phenolic compounds [6], hydrogen peroxide [7], and thiol compounds such as cysteine, glutathione, and thiolcholine [8,9]. CNTs also possess high surface area and have been used to facilitate immobilization of biological molecules [10–12] and for biosensor applications [13–15].

Another important class of organic material for electronic devices is conducting polymers (CPs). Conducting polymers contain alternating single and double bonds between the carbon atoms in their backbone which provide tunable electronic properties (metallic to insulator), low energy optical transitions, low ionization potential and high electron affinity [16–20]. However, most of these properties depend on the synthesis procedure as well as on the dopant nature [21]. Furthermore, conducting polymers exhibit poor mechanical strength. To this end, CNTs doped CP nanocomposites have been explored to improve the mechanical and electrical properties of CPs [22–27].

The use of CNTs for promising applications of biosensors, bio-fuel cells, etc., is made difficult due to their poor solubility in most solvents [28,29]. Of the several methods reported for the solubilization of CNTs, non-covalent functionalization is promising because of the simplicity and as it does not affect the structure of CNTs [30]. In the present work, we report for the first time a simple and mild method to bio-functionalize and solubilize single-walled CNTs (SWNTs) in a single step based on non-covalent adsorption of proteins on to SWNT and the incorporation of the SWNT-protein conjugates in polypyrrole as sole anionic dopant to make nanocomposites for biosensing applications. This unique method has potential for other important applications such as bio-fuel cells.

* Corresponding author. Tel.: +1 951 827 6419; fax: +1 951 827 6419.
E-mail address: adani@engr.ucr.edu (A. Mulchandani).
[1] These authors have contributed equally to the work.

0039-9140/$ – see front matter © 2007 Elsevier B.V. All rights reserved.
doi:10.1016/j.talanta.2007.08.047

2. Experimental

2.1. Materials

Single-walled carbon nanotubes with low functionality, sold under the trade name of P2-SWNT, were provided by Carbon Solutions, Inc. (Riverside, CA, USA). Bovine serum albumin (BSA), horseradish peroxidase (HRP), cytochrome *c* (Cytc), and pyrrole monomer were purchased from Sigma–Aldrich (Milwaukee, WI) and all other chemicals and supplies were purchased from Fisher Scientific (Tustin, CA, USA).

2.2. Solubilization/dispersion of SWNTs with proteins and purification of SWCNT-protein conjugate

One milligram per milliliter of SWNTs and 5 mg/ml of protein (i.e. BSA, HRP, or Cytc) were dissolved in deionized H_2O. The mixture was sonicated for 20 min and then centrifuged for 5 min at 13800 × *g*.

Gel chromatography was used to purify the SWNT-protein conjugate from excess protein. Sephadex G-150 that was presoaked and deaerated using a vacuum pump was packed up to 16 cm in a 2.5 cm diameter × 22 cm long glass column. The SWNT-protein supernatant recovered after centrifugation was layered on the top of the gel and eluted using water flowing under gravity. Volume fractions were collected for 1 min duration using a Bio-Rad model 2110 fraction collector (Bio-Rad Laboratories, Hercules, CA, USA) and analyzed for the presence of SWNTs by measuring absorbance at 500 nm using spectrophotometer (Cary 1E, Varian Inc., Melbourne, Australia) and protein by the Bradford protein assay (Bio-Rad Laboratories, Hercules, CA, USA) and/or absorbance at 280 nm for BSA and 405 nm corresponding to heme for HRP and cytochrome *c*. Fractions showing high absorbance at 725 nm and protein content were pooled for further use.

2.3. Characterization of SWNT-protein conjugate and PPy/SWNT-protein nanocomposite

Scanning electron microscopy (Leo SUPRA 55, Carl Zeiss, Germany) and atomic force microscopy (Nanoscope E and associated equipments, Veeco Instruments, Inc. San Clemente, CA, USA) were used for investigation of the surface morphology.

Vis–NIR absorption spectra for the SWNT-protein conjugate were measured using Mikropack DH-2000 UV–Vis–NIR Light Source and Ocean Optics HR4000 High Resolution Spectrometer (Ocean Optics Inc., Dunedin, FL, USA) using a quartz cuvette.

2.4. Electropolymerization and H_2O_2 detection

Pyrrole was added to the SWNT-protein conjugate pooled fractions for a final concentration of 0.5 M. The mixture was sonicated for 15 min, the pH adjusted to 7 and then purged with nitrogen gas for 10 min for deaeration.

The electropolymerization was performed using cyclic voltammetry (CV) from −0.65 to 1.05 V for 50 cycles using a multi potentio/galvanostat (VMP2, Princeton Applied Research, Oak Ridge, TN, USA). Three electrode configurations were used for electropolymerization where a polished glassy carbon electrode, platinum wire and Ag/AgCl in 3 M KCl were used as working, counter and reference electrode, respectively. The scan rate was fixed at 50 mV/s.

After the electropolymerization, the PPy/SWNT-protein thin film was subjected to overoxidation by cycling the potential from −0.2 to 1.3 V for 50 cycles at 100 mV/s in a deaerated phosphate buffer solution. The overoxidized film was tested for response to 5×10^{-3} M hydrogen peroxide at varying potential from −0.3 to 0.2 V vs. Ag/AgCl reference electrode using a BASi Amperometric Detector (LC-4C, BASi Inc., West Lafayette, IN, USA).

3. Results and discussion

3.1. Solubilization/dispersion of SWNTs with proteins

In an aqueous environment, pristine SWNTs aggregated and settled down at the bottom of the vial (Fig. 1, left), but with the addition of BSA, the SWNTs appeared well dispersed in a suspension (Fig. 1, right). This SWNT-BSA conjugate was stable for well over 2 weeks at room temperature. It has been demonstrated that nonspecific binding occurs between the hydrophobic surface region of a protein and the side wall of a SWNT [31]. With proteins adsorbed on the surface of the SWNT, the SWNT-protein became more water soluble as the surface of the nanostructures became more hydrophilic. This is in agreement with other published work [32]. HRP also displayed similar results whereas Cytc was visually inconclusive and would be verified in a subsequent analytical experiment. The solubilization of SWNT by protein adsorption opens a facile and mild route

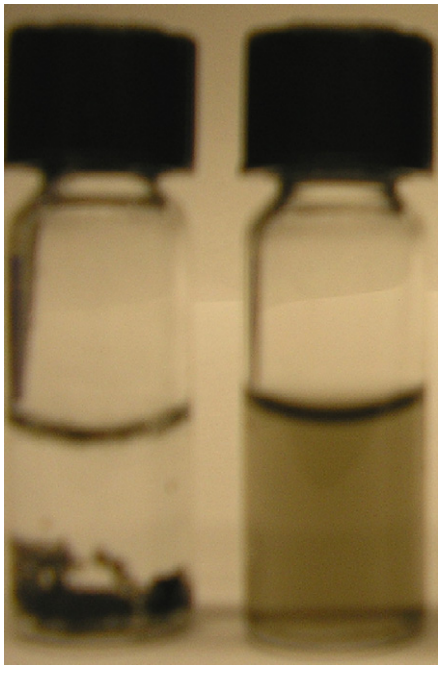

Fig. 1. Photograph of pristine SWNTs (left vial) and SWNT-BSA (right vial) in an aqueous environment after 2 weeks.

for synthesizing functional SWNT-protein conjugate in comparison to the covalent attachment routes demonstrated to-date. The elimination of harsh chemicals and conditions employed in functionalization of CNTs with biomolecules are the added advantages of the present methodology.

3.2. Characterization of SWNT-protein conjugates

The morphology of SWNT-BSA conjugate was characterized with SEM and AFM. The SEM images (Fig. 2) distinctly differentiated between the highly dispersed state of SWNT-BSA conjugates and the aggregated state of pristine SWNTs. The AFM image (Fig. 3) of a single SWNT-BSA conjugate structure showed numerous globular structures binding to a linear structure potentially consisting of multiple SWNTs. The length and diameter of the structure in the AFM image suggested that there were multiple SWNTs since the dimensions of the entire structure were well over the typical length and diameter of a single SWNT. It was very likely that the hydrophobic side walls of several SWNTs bound to each other in a stacking manner as well as to the hydrophobic surface of the proteins. The size of the globular structures from the AFM image also indicated numerous BSA proteins amassing together. These images confirmed the formation of SWNT-protein conjugate.

The amounts of CNTs dispersed can be determined from the absorbance in either the visible range at 500 nm or in the near-

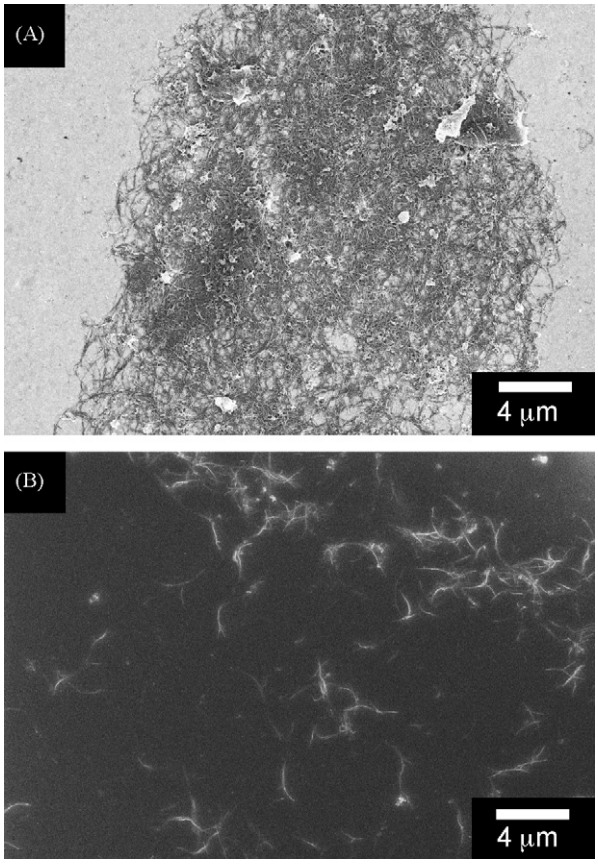

Fig. 2. SEM images of pristine SWNTs (A) and SWNT-BSA conjugates (B).

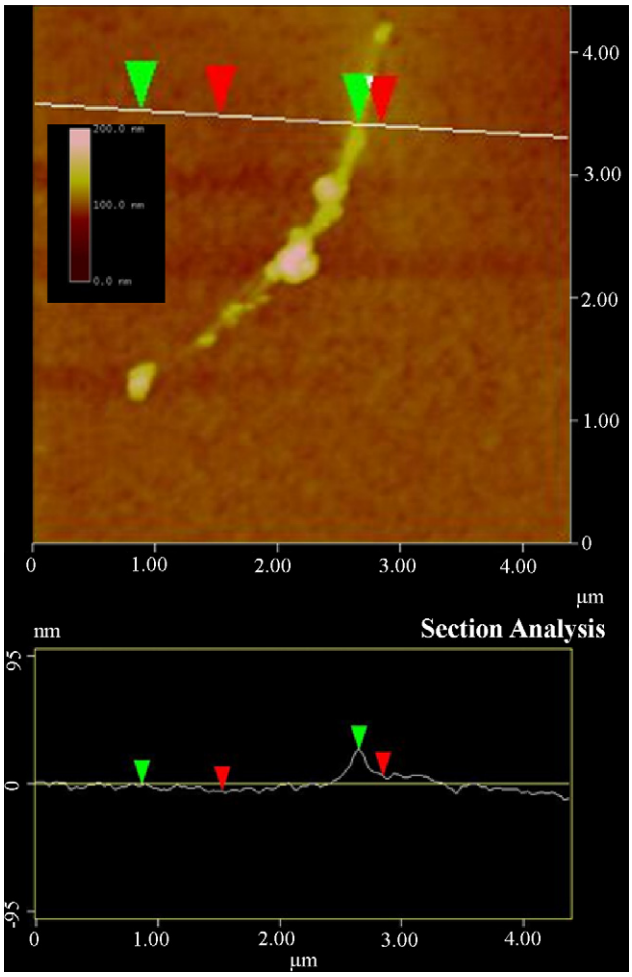

Fig. 3. AFM image of SWCNT-protein conjugate.

infra red region at 1025 nm [33,34]. While the absorbance in the visible range has no specific attribute to any CNT property, the NIR absorbance is a characteristic of the SWNTs relating to the S_{22} interband transition. The absorbance of the SWNT-protein dispersion at both wavelengths indicated the presence of SWNTs in the dispersion and the trend of decreasing solubility in the order of BSA > HRP > cytochrome *c*. Based on 1025 nm absorbance, for which there is no reported extinction coefficient, the SWNT-BSA was approximately five times more soluble than SWNT-HRP, whereas SWNT-cytochrome *c* was very weakly soluble while solubility calculated based on the reported extinction coefficient of 28.6 $L\,g^{-1}\,cm^{-1}$ for HiPco SWNT [35] at 500 nm the solubility were 52.4, 21.3 and 3.8 mg/L for SWNT-BSA, SWNT-HRP and SWNT-Cytc, respectively (Fig. 4). The drastic difference in solubility can be attributed to a varying level of hydrophobic interaction between the proteins and the SWNTs resulting in a varying amount of solubilized SWNTs. If a protein does not have a sufficiently large surface area of hydrophobic groove on its surface, then the level of hydrophobic interaction with SWNTs can be significantly reduced and thus negatively affect the solubilization via non-covalent functionalization. The predominant absorbance peak at 405 nm for HRP and cytochrome *c* is attributed to the heme

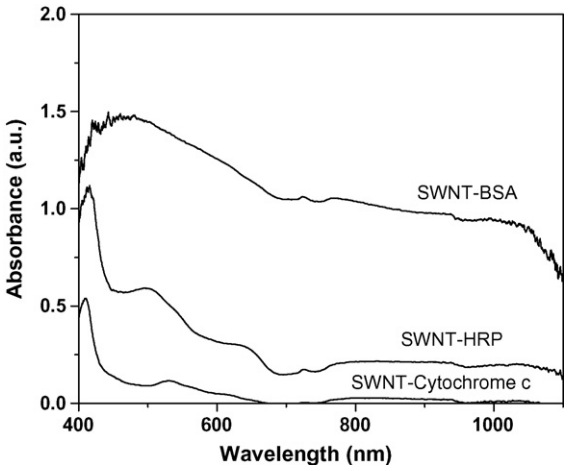

Fig. 4. Vis–NIR absorption spectra of SWNT-proteins.

in these proteins and is an additional confirmation of the presence of these proteins in the conjugates and the concentration trend.

3.3. Electropolymerization of PPy with SWNT-protein conjugate as dopant

CNTs solubilized by introducing –COOH groups or by covalent attachment of poly(*m*-aminobenzene sulfonic acid) have been used as a dopant in polypyrrole film to improve the conductivity and mechanical strength of the film [27,36]. In this work, SWNT solubilized through protein adsorption was applied as the dopant instead. Since the p*I* of BSA is around 4.7 and the p*I* of the 7 isozymes of HRP is reported to be between 3 and 9, both SWNT-proteins conjugates can have overall net negative charges at the pH 7 used for electrochemical polymerization which would allow SWNT-protein conjugates to act as dopants in a polypyrrole film. Pyrrole was added to the purified SWNT-protein suspension and electropolymerized into a film using cyclic voltammetry (Fig. 5). The CVs exhibited typical growth behaviors of an electropolymerization process with a pronounced reduction peak. Because no electrolyte has been added into the deposition bath, SWNT-protein was acting as both an electrolyte and a dopant during the electropolymerization process. The current was much lower during the growth in comparison to the PPy/Cl film because of the higher conductivity and concentration of Cl^- anion compared to the SWNT-protein conjugate. SWNT-cytochrome *c* was not used in this experiment because of the very low concentration. For SWNT-cytochrome *c* conjugate to act as dopant, the electropolymerization would have to be performed at pH above 11 because the p*I* of cytochrome *c* is in the range of 10.37–10.80.

As shown in Fig. 6, the surface morphology of the PPy films differed remarkably between the PPy/SWNT-BSA and PPy/Cl films. SEM image of PPy/SWNT-BSA film revealed a very fibrous three-dimensional reticular structure with interlocking pores whereas the image of PPy/Cl displayed a typical smooth and cauliflower morphology. As the solubilized SWNT-BSAs were being integrated into the polypyrrole film during the electropolymerization process, polypyrrole also coated the surfaces of these conjugates and produced these fibrous structures on the film. These images further verified that SWNT-BSA have been embedded in the polymer matrix as a dopant. The fibrous nature of the film allows the film to be more porous with increased surface area, which would reduce the mass transfer limitation compared to a thick polypyrrole film. Having a larger surface area and lower mass transfer limitation facilitating easier access

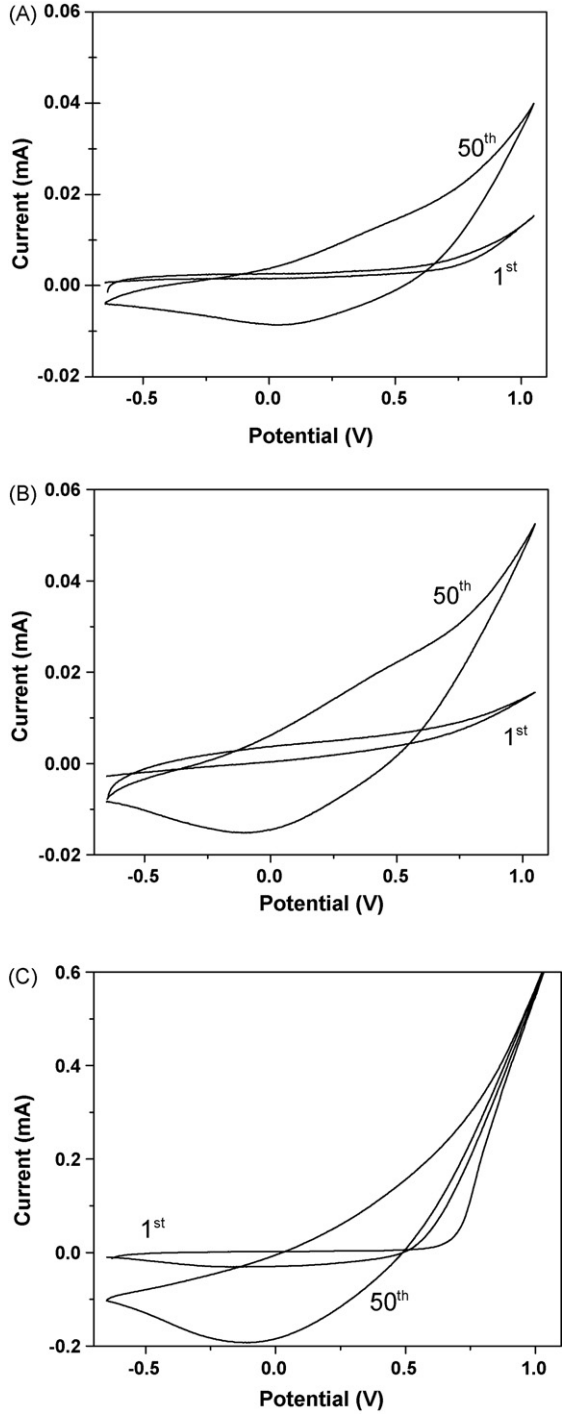

Fig. 5. Potentiodynamic electropolymerization of PPy with (A) SWNT-BSA, (B) SWNT-HRP, and (C) Cl^- as dopants. Pyrrole concentration was fixed at 0.5 M. The scan rate was at 50 mV/s for 50 cycles.

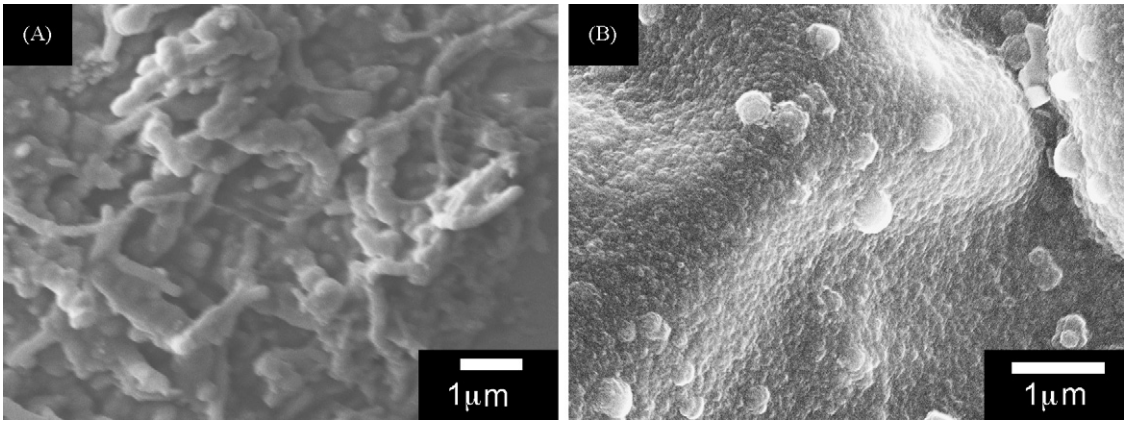

Fig. 6. SEM images of (A) PPy/SWNT-BSA and (B) PPy/Cl^- thin films.

to substrate are favorable for many engineering applications such as fuel cells, in addition to the sensor application demonstrated in the current work.

3.4. Application of SWNT-HRP conjugate doped polypyrrole composite

Recent studies have shown that CNTs can enhance electrochemical reactivity of biomolecules and promote electron transfer reactions of proteins. To evaluate the potential of SWNT-protein doped polypyrrole film for biosensor, we studied the response to H_2O_2 of PPy/SWNT-HRP nanocomposites film and compared to the response of the PPy film in which the HRP (no SWNT) was entrapped during the electropolymerization with chloride dopant by performing hydrodynamic voltammetry (HDV). Since PPy is conducting and also has reducing power and can interfere in the signal from the interaction of the SWNT-HRP or HRP with hydrogen peroxide, the films were overoxidized to render them non-conducting/insulating. As shown in Fig. 7, the CVs for both films at the end of the overoxidation appeared identical in phosphate buffer solution transforming the polypyrrole matrix insensitive to H_2O_2 and thereby allowing the measured signal to be originated from the reduction of H_2O_2 by SWNT-HRP or HRP only.

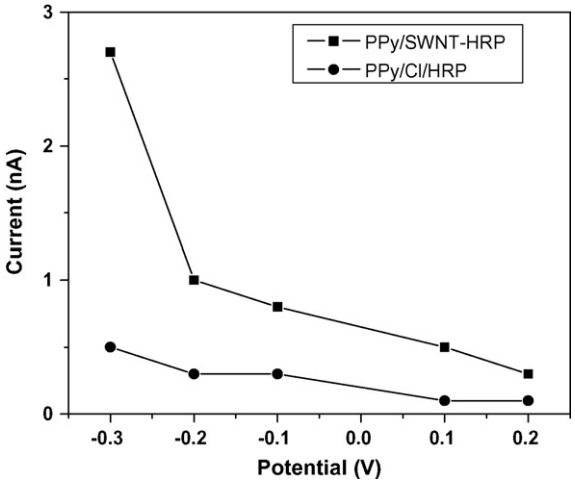

Fig. 8. Hydrodynamic voltammogram of PPy/SWCNT-HRP and PPy/Cl^-/HRP films with 5 mM H_2O_2 as the analyte.

Fig. 8 shows a comparison of the response of PPy/SWCNT-HRP and PPy/Cl/HRP modified electrodes as a function of applied potential to 5 mM H_2O_2. The output current over the full range of potential for the SWNT-HRP doped PPy was higher than for the HRP modified chloride doped PPy. The results show specifically at −0.3 V, the improvement in response was well

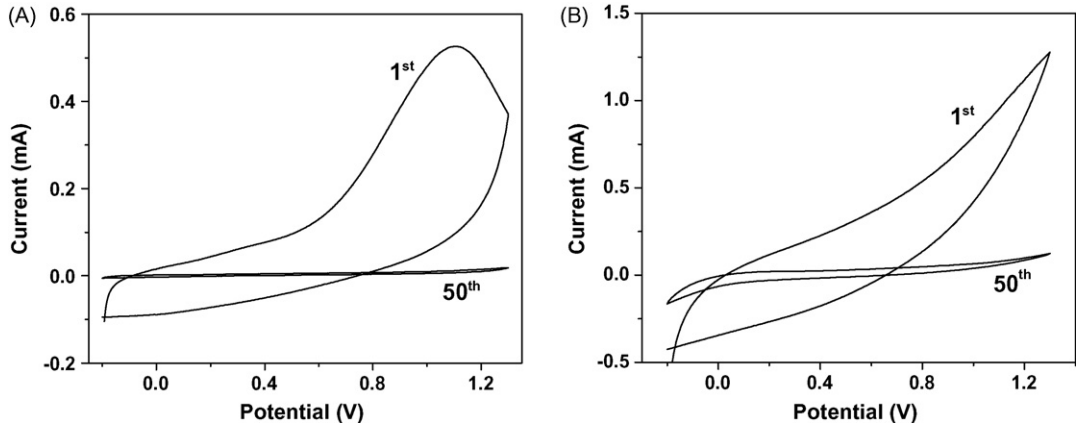

Fig. 7. Overoxidation of (A) PPy/SWNT-HRP and (B) PPy/Cl^-/HRP films.

over 5-fold in comparison against the PPy/Cl/HRP film. The enhanced response can be attributed to several factors. First, the enhanced electron transfer within the polypyrrole matrix from the presence of SWNTs. Second, the direct electron transfer from the active site of the enzymes to the electrode through the SWNT bridging them. Third, improved accessibility of the enzyme catalytic sites for the substrate due to highly open reticular morphology of the nanocomposite film. Lastly, the increased loading of the HRP in the film resulting from the incorporation of SWNT-protein as a dopant and improved efficiency of protein immobilization by adsorption on the SWNTs over the conventional method of entrapment in the film.

4. Conclusion

We demonstrated for the first time a simple and benign method for one-step solubilization and functionalization of CNTs through adsorption under mild/benign conditions and the application of the SWCNT-protein conjugates as dopants for the facile synthesis of SWNT-protein-polypyrrole nanocomposites by electrochemical polymerization. The resulting nanocomposites demonstrated enhanced sensor performance when compared to film with entrapped enzyme. Such strategy potentially can be employed for other biosensors and bio-fuel cell applications by simply substituting another protein.

Congratulation/commemoration

Dear Joe, Here's wishing you happiness and many wonderful moments! Cheers to you! Have a very happy 60th birthday!

Acknowledgements

We acknowledge the support of this work grants CBET-0529330 from the NSF, DMEA90-02-2-0216 from DOD/DARPA/DMEA, and GR-83237501 from the U.S. EPA. M.C. Kum thanks the University of California Toxic Substance Research and Training Program for the fellowship. We thank Prof. Robert Haddon for the SWNTs, Prof. Umar Mohideen and his graduate student Mr. Wei Liu for the AFM images, and Mr. Mangesh Bangar for the SEM imaging.

References

[1] R.H. Baughman, A.A. Zakhidov, W.A. de Heer, Science 297 (2002) 787–792.
[2] N. Li, J. Wang, M. Li, Rev. Anal. Chem. 22 (2003) 19–33.
[3] B.S. Sherigara, W. Kutner, F. D'Souza, Electroanalysis 15 (2003) 753–772.
[4] H. Luo, Z. Shi, N. Li, Z. Gu, Q. Zhuang, Anal. Chem. 73 (2001) 915–920.
[5] M. Musameh, J. Wang, A. Merkoci, Y. Lin, Electrochem. Commun. 4 (2002) 743–746.
[6] J. Wang, R.P. Deo, M. Musameh, Electroanalysis 15 (2003) 1830–1834.
[7] J. Wang, M. Musameh, Y. Lin, J. Am. Chem. Soc. 125 (2003) 2408–2409.
[8] X.N. Cao, L. Lin, Y.Z. Xian, W. Zhang, Y.F. Xie, L.T. Jin, Electroanalysis 15 (2003) 892–897.
[9] K.A. Joshi, J. Tang, R. Haddon, J. Wang, W. Chen, A. Mulchandani, Electroanalysis 17 (2005) 54–58.
[10] R.J. Chen, Y. Zhang, D. Wang, H. Dai, J. Am. Chem. Soc. 123 (2001) 3838–3839.
[11] J.J. Davis, M.L.H. Green, H.A.O. Hill, Y.C. Leung, P.J. Sadler, J. Sloan, A.V. Xavier, S.C. Tsang, Inorg. Chim. Acta 272 (1998) 261–266.
[12] F. Balavoine, P. Schultz, C. Richard, V. Mallouh, T.W. Ebbesen, C. Mioskowski, Angew. Chem., Int. Ed. 38 (1999) 1912–1915.
[13] Y. Lin, F. Lu, J. Wang, Electroanalysis 16 (2004) 145–149.
[14] A. Guiseppi-Elie, C. Lei, R.H. Baughman, Nanotechnology 13 (2002) 559–564.
[15] R.P. Deo, J. Wang, I. Block, A. Mulchandani, K.A. Joshi, M. Trojanowicz, F. Scholz, W. Chen, Y. Lin, Anal. Chim. Acta 530 (2005) 185–189.
[16] E. Smela, N. Gadegaard, Adv. Mater. 11 (1999) 953–957.
[17] A.G. MacDiarmid, Angew. Chem. Int. Ed. 40 (2001) 2581–2590.
[18] V. Saxena, B.D. Malhotra, Curr. Appl. Phys. 3 (2003) 293–305.
[19] T.F. Otero, I. Boyano, M.T. Cortéz, G. Vázquez, Electrochim. Acta 49 (2004) 3719–3726.
[20] L. Dai, P. Soundarrajan, T. Kim, Pure Appl. Chem. 74 (2002) 1753–1772.
[21] A. Ramanaviciene, A. Ramanavicius, in: D.W. Thomas (Ed.), Advanced Biomaterials for Medical Applications, Kluwer Academic Publishers, Netherlands, 2004, p. 111.
[22] M. Hughes, G.Z. Chen, M.S.P. Shaffer, D.J. Fray, A.H. Windle, Chem. Mater. 14 (2002) 1610–1613.
[23] C. Downs, J. Nugent, P.M. Ajayan, D.J. Duquette, K.S.V. Santhanam, Adv. Mater. 11 (1999) 1028–1031.
[24] M. Gao, S. Huang, L. Dai, G. Wallace, R. Gao, Z. Wang, Angew. Chem., Int. Ed. 39 (2000) 3664–3667.
[25] Z. Wei, M. Wan, T. Lin, L. Dai, Adv. Mater. 15 (2003) 136–139.
[26] H. Zengin, W. Zhou, J. Jin, R. Czerw, D.W. Smith Jr., L. Echegoyen, D.L. Carroll, S.H. Foulger, J. Ballato, Adv. Mater. 14 (2002) 1480–1483.
[27] G.Z. Chen, M.S.P. Shaffer, D. Coleby, G. Dixon, W. Zhou, D.J. Fray, A.H. Windle, Adv. Mater. 12 (2000) 522–526.
[28] A. Star, J.F. Stoddart, D. Steuerman, M. Diehl, A. Boukai, E.W. Wong, X. Yang, S.W. Chung, H. Choi, J.R. heath, Angew. Chem., Int. Ed. 40 (2001) 1721–1725.
[29] J. Chen, M.A. Hamon, H. Hu, Y. Chen, A.M. Rao, P.C. Eklund, R.C. Haddon, Science 282 (1998) 95–98.
[30] M.J. O'Connell, P. Boul, L.M. Ericson, C. Huffman, Y. Wang, E. Haroz, C. Kuper, J. Tour, K.D. Ausman, R.E. Smalley, Chem. Phys. Lett. 342 (2001) 265–271.
[31] R.J. Chen, S. Bangsaruntip, K.A. Drouvalakis, N.W.S. Kim, M. Shim, Y. Li, W. Kim, P.J. Utz, H. Dai, Proc. Natl. Acad. Sci. U.S.A. 100 (2003) 4984–4989.
[32] S.S. Karajanagi, H. Yang, P. Asuri, E. Sellitto, J.S. Dordick, R.S. Kane, Langmuir 22 (2006) 1392–1395.
[33] B. Zhao, H. Hu, A. Yu, D. Perea, R.C. Haddon, J. Am. Chem. Soc. 127 (2005) 8197–8203.
[34] P. Asuri, S.S. Karajanagi, E. Sellitto, D.-Y. Kim, R.S. Kane, J.S. Dordick, Biotechnol. Bioeng. (2006) 804–811.
[35] J. Bhar, E.T. Mickelson, M.J. Bronikowski, R.E. Smalley, J.M. Tour, Chem. Commun. (2001) 93–194.
[36] A.K. Wanekaya, Y. Lei, E. Bekyarova, W. Chen, R. Haddon, A. Mulchandani, N.V. Myung, Electroanalysis 18 (2006) 1047–1054.